Annexin A1–containing extracellular vesicles and polymeric nanoparticles promote epithelial wound repair

Giovanna Leoni,[1,2] Philipp-Alexander Neumann,[1,3] Nazila Kamaly,[4] Miguel Quiros,[1] Hikaru Nishio,[1] Hefin R. Jones,[5] Ronen Sumagin,[1] Roland S. Hilgarth,[1] Ashfaqul Alam,[1] Gabrielle Fredman,[6] Ioannis Argyris,[3] Emile Rijcken,[3] Dennis Kusters,[7] Chris Reutelingsperger,[7] Mauro Perretti,[5] Charles A. Parkos,[1,8] Omid C. Farokhzad,[4] Andrew S. Neish,[1] and Asma Nusrat[1]

[1]Epithelial Pathobiology and Mucosal Inflammation Research Unit, Department of Pathology and Laboratory Medicine, Emory University School of Medicine, Atlanta, Georgia, USA. [2]Institute for Cardiovascular Prevention, Ludwig-Maximilians-University, Munich, Germany. [3]Department of General and Visceral Surgery, University Clinic of Muenster, Muenster, Germany. [4]Laboratory of Nanomedicine and Biomaterials, Department of Anesthesiology, Brigham and Women's Hospital, Harvard Medical School, Boston, Massachusetts, USA. [5]William Harvey Research Institute, Barts and The London School of Medicine, Queen Mary University of London, London, United Kingdom. [6]Departments of Medicine, Pathology and Cell Biology, and Physiology, Columbia University, New York, New York, USA. [7]Cardiovascular Research Institute Maastricht, Department of Biochemistry, Maastricht University, Maastricht, Netherlands. [8]Department of Pathology, University of Michigan, Ann Arbor, Michigan, USA.

Epithelial restitution is an essential process that is required to repair barrier function at mucosal surfaces following injury. Prolonged breaches in epithelial barrier function result in inflammation and further damage; therefore, a better understanding of the epithelial restitution process has potential for improving the development of therapeutics. In this work, we demonstrate that endogenous annexin A1 (ANXA1) is released as a component of extracellular vesicles (EVs) derived from intestinal epithelial cells, and these ANXA1-containing EVs activate wound repair circuits. Compared with healthy controls, patients with active inflammatory bowel disease had elevated levels of secreted ANXA1-containing EVs in sera, indicating that ANXA1-containing EVs are systemically distributed in response to the inflammatory process and could potentially serve as a biomarker of intestinal mucosal inflammation. Local intestinal delivery of an exogenous ANXA1 mimetic peptide (Ac2-26) encapsulated within targeted polymeric nanoparticles (Ac2-26 Col IV NPs) accelerated healing of murine colonic wounds after biopsy-induced injury. Moreover, one-time systemic administration of Ac2-26 Col IV NPs accelerated recovery following experimentally induced colitis. Together, our results suggest that local delivery of proresolving peptides encapsulated within nanoparticles may represent a potential therapeutic strategy for clinical situations characterized by chronic mucosal injury, such as is seen in patients with IBD.

Introduction

The gastrointestinal epithelium functions as a dynamic and selective barrier, which plays an important role in limiting the access of luminal contents to the mucosal and systemic immune system. Epithelial injury results in compromised barrier function, as seen in pathologic states that are associated with mucosal inflammation. A major consequence of the breeched epithelial barrier is exposure of immunocompetent subepithelial lamina propria cells to luminal antigens and bacteria. This results in local recruitment of leukocytes and generation of proresolving mediators that orchestrate resolution of inflammation and ultimately epithelial repair. Thus, healing of epithelial wounds represents active coordination of proresolving mediators and repair events, wherein platelets, fibroblasts, and epithelial, endothelial, and inflammatory cells act together to restore the epithelial barrier and reestablish mucosal homeostasis (1). Recent studies have highlighted a critical role of secreted lipids and proteins in facilitating epithelial wound repair. Such proresolving mediators include lipoxins, resolvins, protectins, maresins, prostaglandins, cytokines, and annexin A1 (ANXA1) (2, 3).

ANXA1 facilitates resolution of inflammation by binding to formyl peptide receptors (FPRs) expressed on responsive cells, such as phagocytes and epithelial cells (4–6). We have previously shown that ANXA1 stimulates intestinal mucosal wound repair in a murine model of colitis (7). However, the mechanism by which this cytosolic protein activates prorestitutive signaling after injury is not understood. Furthermore, the mechanics of how ANXA1 itself is regulated remain to be defined.

Neutrophils express ANXA1, and recent studies have demonstrated that ANXA1 is released from them as a component of extracellular vesicles (EVs) (8, 9). EVs are subclassified into exosomes and microparticles (10). Exosomes are 40 to 60 nm in size and are produced by dendritic cells, macrophages, epithelial cells, and a variety of tumor cells. They are formed by membrane

Authorship note: Giovanna Leoni, Philipp-Alexander Neumann, and Nazila Kamaly contributed equally to this work.

Conflict of interest: Omid C. Farokhzad discloses his financial interest in BIND Biosciences, Selecta Biosciences, and Blend Therapeutics, three biotechnology companies developing nanoparticle technologies for medical applications. BIND Biosciences, Selecta Biosciences, and Blend Therapeutics did not support the aforementioned research, and currently, these companies have no rights to any technology or intellectual property developed as part of this research.

Submitted: April 21, 2014; **Accepted:** January 2, 2015.

Reference information: *J Clin Invest*. 2015;125(3):1215–1227. doi:10.1172/JCI76693.

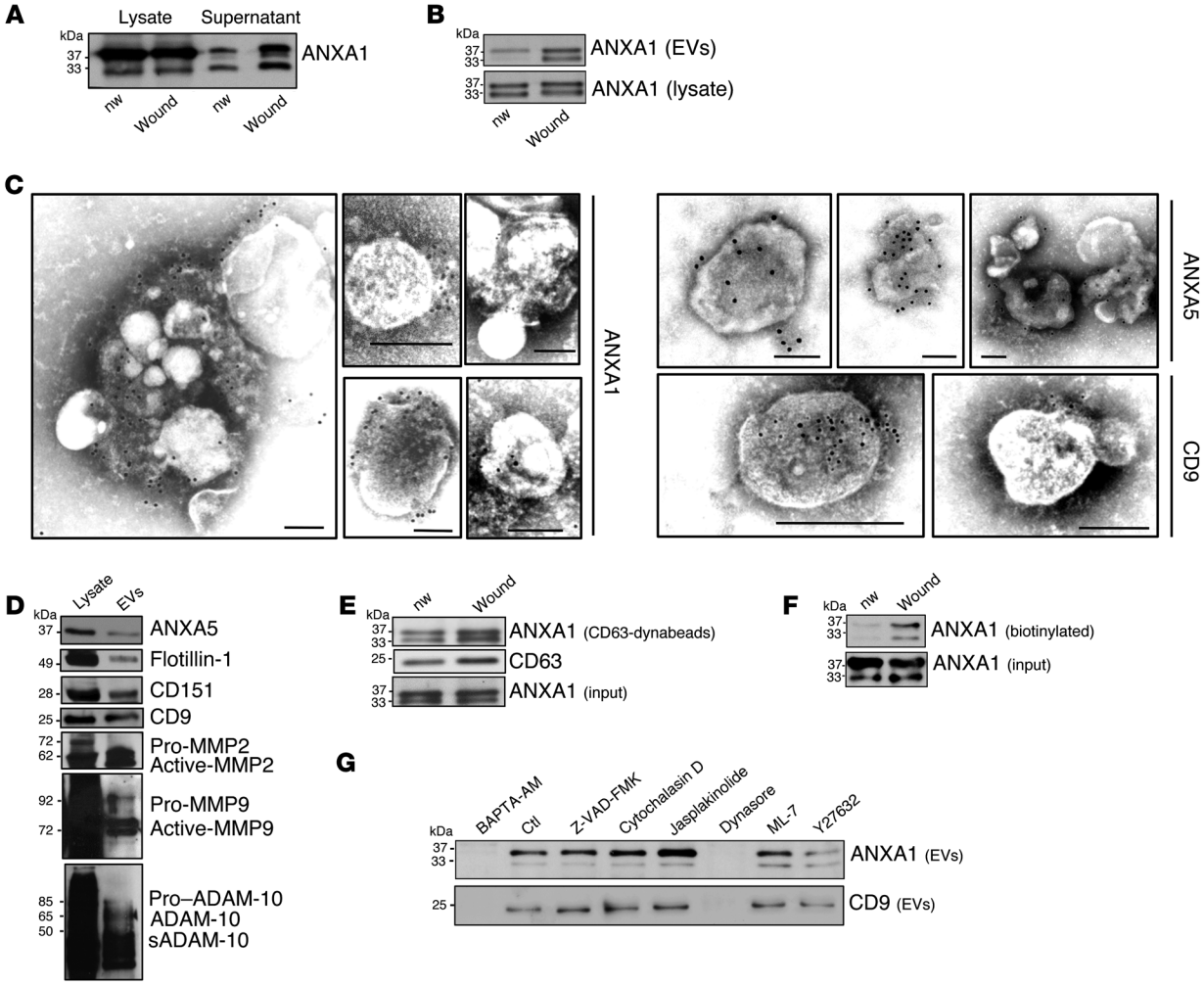

Figure 1. Intestinal epithelial wounding induces release of ANXA1-bearing EVs. (**A**) Immunoblotting for ANXA1 protein in supernatant of nonwounded (nw) or wounded (wound) human epithelial cells. Densitometry analysis shows that ANXA1 protein in cell supernatants derived from wounded cells is significantly increased versus nonwounded confluent cells (2.94-fold increase, $P < 0.0001$, average of $n = 5$ immunoblots), and no significant change was observed in the lysate. (**B**) Immunoblotting for ANXA1 protein in EVs isolated from supernatant. Densitometry analysis shows that ANXA1 protein on EVs derived from wounded cells is increased versus nonwounded cells (2.166-fold increase, $P = 0.0066$, average of $n = 4$ immunoblots). (**C**) Immunogold labeling for ANXA1 and transmission electron microscopy to detect ANXA1 distribution in EVs. Scale bar: 100 nm. (**D**) Immunoblotting for conventional EV markers in epithelial cell lysates (representative of $n = 4$ immunoblots). sADAM-10, soluble ADAM-10. (**E**) EVs were incubated with $CD63^+$ Dynabeads and analyzed by immunoblotting. Densitometry analysis shows that ANXA1 protein on EVs derived from wounded cells is increased versus nonwounded cells (1.459-fold increase, $P = 0.0004$, average of $n = 4$ immunoblots). (**F**) Biotinylated cell surface proteins released from the supernatant of nonwounded and wounded IECs captured with avidin sepharose beads. Densitometry analysis shows that ANXA1 protein on EVs derived from wounded cells is increased versus nonwounded cells (4.239-fold increase increase, $P = 0.0002$, average of $n = 4$ immunoblots). (**G**) Immunoblots show ANXA1 and CD9 proteins in EVs after IEC wounding and treatment with BAPTA-AM (30 μM), Z-VAD-FMK (25 mM), cytochalasin D (2 μM), jasplakinolide (1 μM), dynasore (80 μM), ML-7 (20 μM), and Y-27632 (10 μM). All the results in this figure are representative of at least 3 independent experiments.

invaginations and are released when intracellular vesicles combine with a multivesicular body, which then fuses with the plasma membrane and results in exocytosis (10). Membrane-bound proteins most commonly associated with exosomes include tetraspanins, specifically CD9 and CD63, which have been used in previous studies as markers of intestinal epithelial-derived exosomes (11, 12). In contrast to exosomes, microparticles are larger (100 to 1,000 nm) and are released by plasma membrane shedding via a processes also referred to as ectocytosis (13). EVs can either disperse in the extracellular space near the site of release or over significant distances, ultimately appearing in biological fluids, such as plasma, serum, and urine (14).

In this work, we demonstrate that epithelial cells release the potent endogenous proresolving mediator ANXA1 as a component of EVs that promote intestinal mucosal wound repair. Furthermore, we investigate the therapeutic wound-healing properties of an ANXA1 mimetic peptide Ac2-26 that is delivered using polymeric nanoparticles (NPs). Since NPs can be synthesized with unique bioavailability and degradation properties, we harnessed the novel prorepair properties of the ANXA1 mimetic peptide Ac2-26 by administering NPs encapsulating this peptide (Ac2-26 Col IV NPs) (15). Remarkably, a single systemic administration of the Ac2-26 Col IV NPs was sufficient in accelerating epithelial barrier repair during the resolution phase of murine colitis. Similarly, a

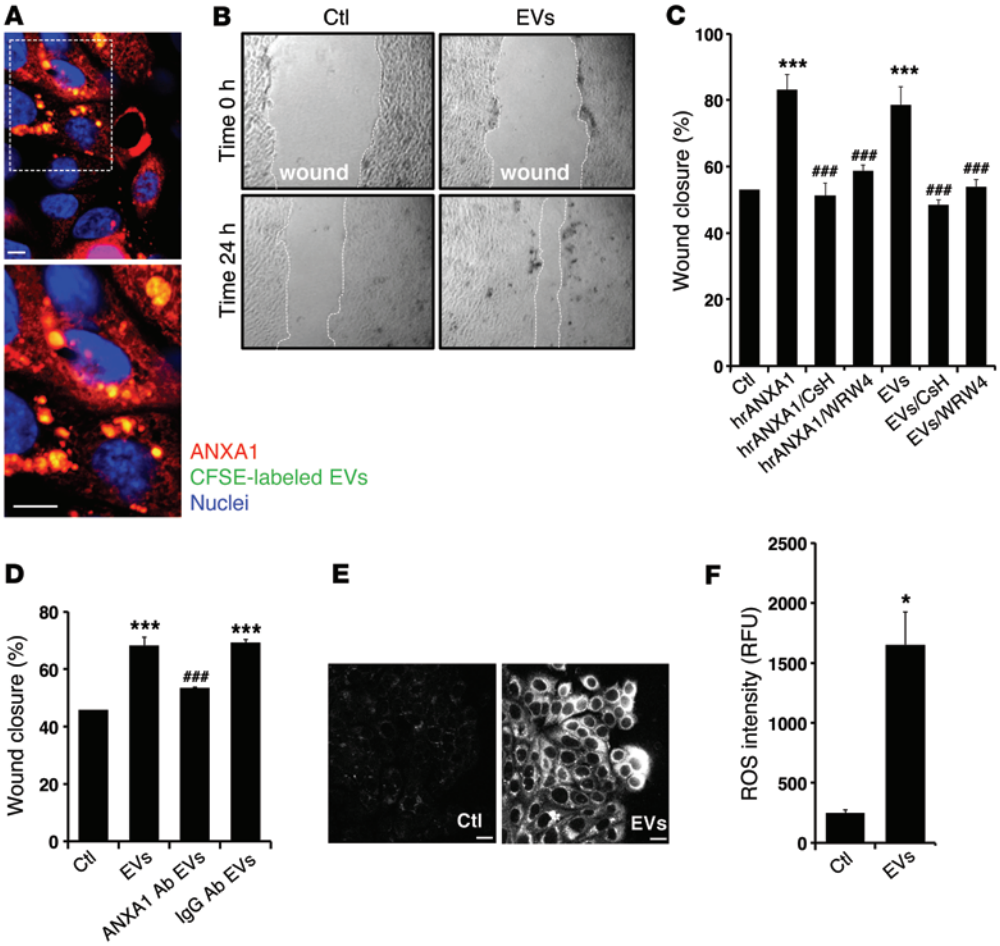

Figure 2. EVs containing ANXA1 regulate epithelial wound healing. (**A**) Representative (of $n = 5$) en face image of migrating IECs after 24 hours of interaction with labeled EVs (CFSE, 10 μmol/l; Molecular Probes). The boxed area (original magnification, ×40) is shown at high magnification in the image below (original magnification, ×100). Scale bar: 10 μm. (**B** and **C**) Scratch wound healing assay using IEC monolayers. EVs and hrANXA1 were added to wounded IECs alone and in the presence of FPR1 antagonist, CsH (1 μM); FPR2/ALX antagonist, WRW4 (10 μM); and other conditions, as indicated. Wound widths were determined at time 0 and 24 hours ($n = 5$, mean ± SEM) (original magnification, ×10). (**D**) Scratch wound healing assay using IEC monolayers. EVs were added to wounded IECs alone and in the presence of mouse monoclonal ANXA1 inhibitory antibody (250 μg/ml) or control IgG antibody (250 μg/ml). The experiments in **C** and **D** were repeated 3 times, and results of one representative experiment performed with 5 parallel samples are shown (mean ± SEM). $^{***}P < 0.0001$ compared with control; $^{###}P < 0.0001$ compared with EVs. (**E** and **F**) IECs were incubated with EVs for 15 minutes, and ROS generation was detected by confocal microscopy using the fluorescent Hydro-Cy3 dye (15 μM). Scale bar: 40 μm. Summarized data for Hydro-Cy3 fluorescence intensity are presented in the graph (mean ± SEM, $^{*}P = 0.0002$ vs. control, $n = 3$). Confocal micrographs are representative of 3 independent experiments. All the results in this figure are representative of at least 3 independent experiments. Statistical comparisons were performed by ANOVA with Tukey's multiple comparison post-test for **C** and **D** and 2-tailed Student's t test for **F**. RFU, relative fluorescent units.

single intramucosal injection of Ac2-26 Col IV NPs promoted closure of intestinal mucosal biopsy-induced wounds. These results indicate that NPs containing prorepair molecules are capable of not only improving resolution of inflammation but also function in accelerating ultimate recovery of the critical epithelial barrier function. Such delivery mechanisms can be used as novel therapeutic approaches to promote mucosal wound repair.

Results

ANXA1 released in intestinal epithelial-derived EVs plays an important role in promoting wound repair. To identify the mechanism by which ANXA1 associated with the inner leaflet of the plasma membrane gains access to extracellular surface FPRs, we first determined whether ANXA1 was released from epithelial cells into the extracellular space. Indeed, as shown in Figure 1A, full-length ANXA1 protein was identified in the supernatants of intestinal epithelial cells (IECs), and increased amounts of ANXA1 were released from the wounded epithelial cell monolayer (Figure 1A). We next sought to identify the protease that mediates ANXA1 cleavage in the extracellular compartment. Since MMPs target extracellular substrates, we examined whether epithelial-derived ANXA1 is cleaved by MMPs after IEC wounding (16). Incubation of epithelial cells with MMP inhibitors (TAPI-2, MMP9-selective inhibitor, and ADAM-10 inhibitor GI254023X) decreased the release of ANXA1 into the cell culture supernatant (Supplemental Figure 1A; supplemental material available online with this article; doi:10.1172/JCI76693DS1). The MMP9-specific inhibitor displayed a significant effect in decreasing ANXA1 release in EVs (Supplemental Figure 1B). To determine whether ANXA1 was released from human IECs as a component of EVs, particles were isolated by ultracentrifugation from epithelial cell culture supernatants derived from either confluent IEC monolayers or resealing wounds in vitro. As shown in the immunoblot in Figure 1B, ANXA1 was not only identified in EVs, but their release was increased during wound closure. ANXA5 and CD9 have previously been shown to reside in EVs (10, 12); therefore, they were used as EVs markers. To further characterize ANXA1-containing EVs, we performed immunogold labeling and electron microscopy of EVs isolated from supernatants of resealing IEC wounds. As shown in Figure 1C, ANXA1, ANXA5, and CD9 were identified in round and cup-shaped vesicles characteristic of exosomes and in larger vesicles consistent with microparticles. The presence of ANXA1 and the composition of EVs were

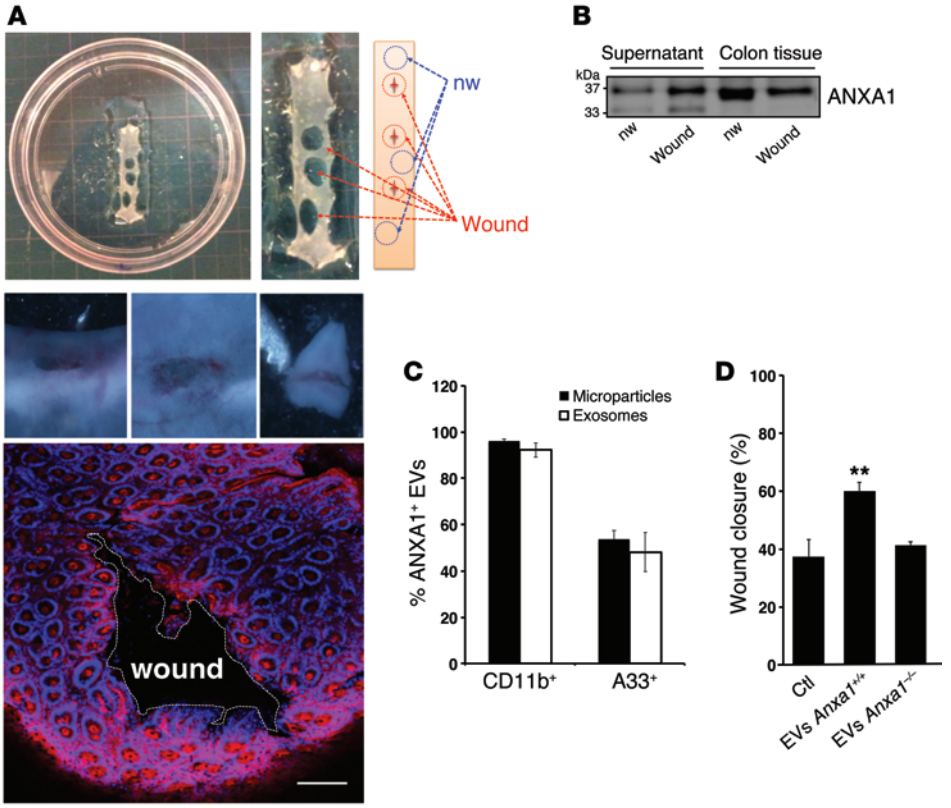

Figure 3. Analysis of ANXA1-containing EVs in ex vivo cultures of resealing mucosal wounds and functional effects of EVs on wound closure. (**A**) 4-mm punch biopsy of resealing colonic wounds (1 day after injury, red circle) and nonwounded mucosa (blue circle) were rinsed in sterile PBS to remove cellular debris and immediately placed into a 24-well culture plate (3 wounds from each mouse per well, $n = 4$). Photographic images of a wound (1- to 2-mm size) and confocal images of resealing mucosal wound showing F-actin (Alexa Fluor 555 phalloidin, pink) and nuclei (TO-PRO-3, blue) are shown ($n = 4$). Scale bar: 100 μm. (**B**) Immunoblot showing ANXA1 in the supernatant and lysate of the ex vivo culture. Densitometry analysis shows that ANXA1 protein in culture supernatants derived from wounded cultures is significantly increased versus nonwounded cells (1.979-fold increase, $P = 0.0024$ average of $n = 3$ immunoblots). In total lysate, the ratio of ANXA1 expression in wounded tissue versus nonwounded tissue is 0.762 ($P = 0.0005$ average of $n = 3$ immunoblots). (**C**) EVs (microparticles and exosomes) were stained with BODIPY-Texas Red and conjugated CD11b, A33, and ANXA1 fluorescent antibodies. Data are expressed as mean ± SEM; $n = 4$ per group. (**D**) EVs derived from *Anxa1*$^{+/+}$ and *Anxa1*$^{-/-}$ mice were added to monolayers of cultured murine epithelial cells, and scratch wound resealing assay was performed. Increased wound closure was observed after incubation with ANXA1-containing EVs (**$P = 0.0025$) compared with EVs lacking ANXA1. Mean ± SEM; $n = 15$ mice per group. Statistical comparisons were performed by ANOVA with Tukey's multiple comparison post-test.

further evaluated by immunoblotting. In addition to ANXA1, ANXA5, CD9, EVs contained other previously reported EV-associated proteins, including flotillin, CD151, MMP2, MMP9, and ADAM-10 (refs. 10, 17, and Figure 1D).

Since the tetraspanin protein CD63 has been reported as a component of exosomes (18), we used ultracentrifugation and bead affinity purification to isolate CD63$^+$ exosomes and subsequently detected ANXA1 by immunoblotting. As shown in Figure 1E, ANXA1 was identified in CD63-containing EVs, and this association was increased in supernatants from resealing IEC wounds. Furthermore, cell surface biotinylation experiments were performed to demonstrate that some of the ANXA1 in EVs was derived from the plasma membrane (Figure 1F).

Having shown that ANXA1 is released as a component of EVs, we investigated the mechanisms that control this process. ANXA1 is a calcium-dependent phospholipid-binding protein, and changes in intracellular calcium concentrations have also been shown to influence generation of EVs (19, 20). Accordingly, we observed that chelation of intracellular calcium with BAPTA-AM reduced EV-associated ANXA1 (Figure 1G). Perturbation of F-actin dynamics with jasplakinolide or cytochalasin D (21) increased ANXA1 expression release in EVs (Figure 1G). Additionally, to study the role of actin myosin contraction, we analyzed Rho-associated kinase (ROCK) and myosin light chain kinase phosphorylation. ROCK inhibition with a small-molecule inhibitor, Y27632, but not with an inhibitor of myosin light chain kinase, ML-7, decreased ANXA1 release in EVs (Figure 1G). Consistently, the dynamin inhibitor, dynasore, decreased ANXA1 association with EVs during wound closure. To exclude the possibility that ANXA1 in IEC supernatants was derived from apoptotic cells, we inhibited apoptosis using a pan-caspase inhibitor (Z-VAD-FMK). Then, we analyzed the amount of ANXA1 by immunoblotting EVs from resealing wounds (Figure 1G) and detected no differences.

To further characterize the EVs obtained from the culture supernatants of IEC lines during the wound closure model, we analyzed EVs by imaging flow cytometry as described recently (22). A detailed analysis of EVs with calibration beads ranging from 1 μm to 50 nm was performed, and EVs were quantified in the supernatants of epithelial cells (Supplemental Figure 1, B–D). Our data revealed that inhibition of ROCK activity (with Y27632 compound) decreased ANXA1-containing EVs, supporting a role of ROCK-mediated actin-myosin contraction in controlling the release of EVs loaded with ANXA1 from epithelial cells (Figure 1G and Supplemental Figure 1C).

To determine whether the release of ANXA1-containing EVs from epithelial cells was altered in inflammatory states, we incubated epithelial cells with proinflammatory cytokines (IL-1β, IFN-γ, and TNF-α). Analysis of cell culture supernatants upon separation by ultracentrifugation indicated that cytokines increased ANXA1 release in the EVs (Supplemental Figure 1D).

Taken together, these results show that ANXA1 release in IEC-derived EVs requires actin-myosin contraction and can be modulated by proinflammatory cytokines.

FPR signaling by ANXA1 in EVs promotes IEC wound closure. To assess the functional effects of ANXA1-containing EVs on epithe-

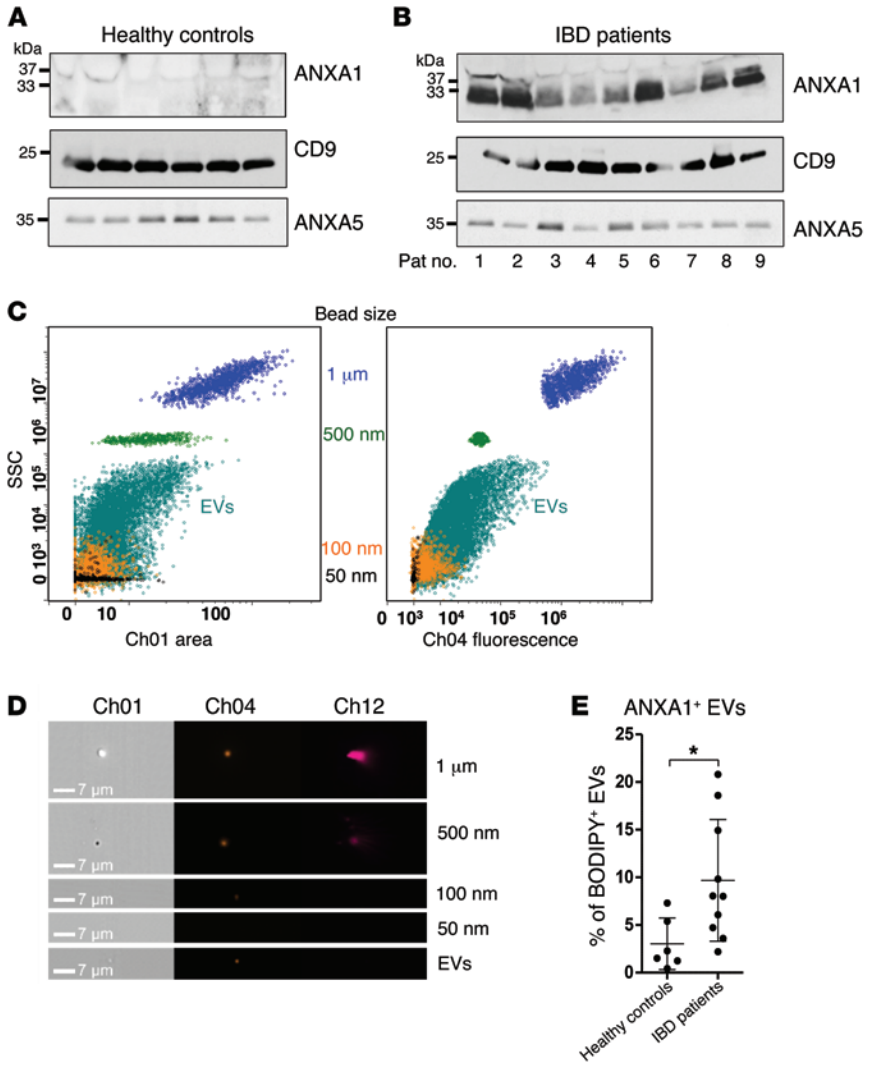

Figure 4. Serum-derived exosomes from healthy controls and patients with IBD. (**A** and **B**) Immunoblots of ANXA1, CD9, and ANXA5 in isolated exosomes from sera of human (**A**) healthy controls and (**B**) patients with IBD. Exosomes were precipitated from human pooled sera using SBI's Serum ExoQuick precipitation reagent (data are representative of $n = 3$ experiments). (**C**) Representative side scatter versus bright-field area (SSC/Ch12) and Ch04 fluorescence plots for EV isolates acquired with 1-μm and 500-nm reference beads (100-nm and 50-nm beads were acquired separately and overlaid) of EVs isolated from human sera by ultracentrifugation ($n = 3$). (**D**) Representative bright-field (Ch01), Ch04, and Ch012 images of each population of beads and EVs ($n = 3$) (original magnification, ×60). Scale bar: 7 μm. (**E**) EVs were stained with BODIPY-Texas Red and conjugated fluorescent antibodies against ANXA1 ($n = 3$). Data are expressed as mean ± SD. $^*P = 0.0194$. Statistical comparisons were performed by 2-tailed Student's t test.

lial wound repair, resealing IEC wounds were incubated with fluorescently labeled EVs (using CFSE) (Figure 2A). Indeed, visualized labeled EVs were associated with epithelial cells and significantly enhanced wound repair ($P < 0.0001$), as shown in Figure 2B. Since FPRs mediate ANXA1 signaling to promote IEC wound repair (4, 7, 23), we examined whether the FPR1 and FPR2/ALX antagonists (CsH and WRW4) influenced ANXA1-containing EV–mediated IEC wound closure. As shown in Figure 2C, inhibition of both receptors abrogated the prohealing effects of ANXA1-containing EVs. Furthermore, incubation of resealing wounds with EVs in the presence of a neutralizing anti-ANXA1 antibody (24), but not control IgG, inhibited EV-mediated increase in wound closure (Figure 2D). Interestingly, another member of the annexin protein family, ANXA5, also identified in epithelial-derived EVs, did not promote wound closure (Supplemental Figure 1E). These findings support a specific role of ANXA1-containing EVs in signaling via FPRs to promote IEC wound healing.

We have previously reported that ANXA1 promotes IEC wound repair by ROS generation mediated by FPR and NOX1 signaling (7). To test whether IEC exposure to ANXA1-containing EVs also induces ROS generation, we visualized superoxide production using the stable and nontoxic redox-sensitive hydrocyanine 3 (Hydro-Cy3) dye, which fluoresces when oxidized (25). As shown in Figure 2, E and F, incubation of resealing wounds with EVs increases ROS generation at the wound edge, consistent with the effects previously observed with the ANXA1 mimetic peptide (7).

To further verify the above in vitro results, we isolated EVs from ex vivo resealing murine intestinal mucosal wounds in wild-type mice (*Anxa1*$^{+/+}$ EVs) and ANXA1-null mice (*Anxa1*$^{-/-}$ EVs). As shown in Supplemental Figure 2B, ANXA1 protein expression was absent in *Anxa1*$^{-/-}$ mice. A total of 3 colonic mucosal biopsy-induced wounds per mouse were obtained (7, 26). Resealing colonic wounds and their adjoining intact mucosa were later harvested for ex vivo culture (Figure 3A). ANXA1 protein in the culture media as well as in murine tissue was analyzed by immunoblotting and by Amnis ImageStream X Mk II imaging flow cytometry. ANXA1 release was higher in supernatants from wounded mucosa of wild-type mice compared with that in nonwounded mucosal tissue 1 day after injury (Figure 3B). This flow cytometry technique identified several EV subtypes (exosomes and microparticles; Figure 3C) in the supernatant of wounded mucosa and elucidated their cell of origin. The vast majority of CD11b$^+$ EVs were positive for ANXA1. The A33 antigen, a transmembrane protein expressed almost exclusively by epithelial cells, was also used to detect

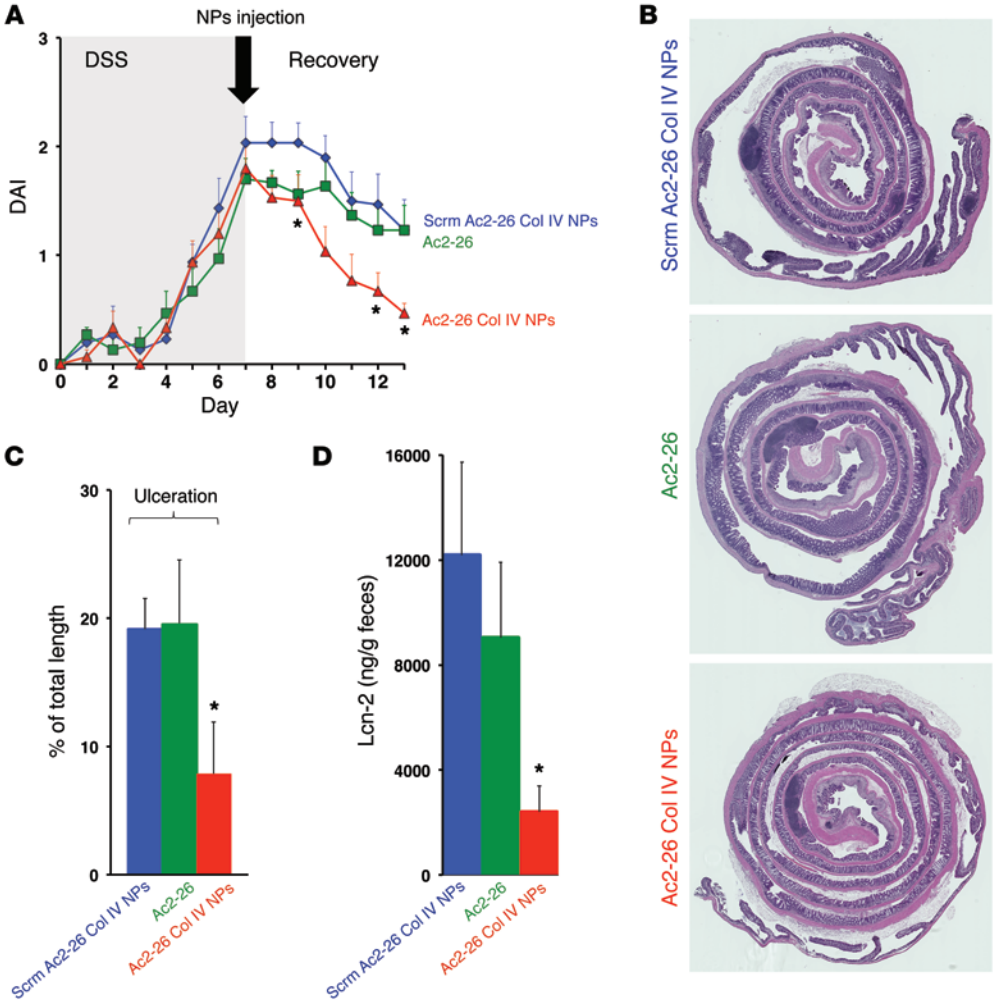

Figure 5. NPs containing Ac2-26 accelerate recovery of murine colitis in vivo. (**A**) Clinical disease activity index (DAI) of *Anxa1*$^{-/-}$ mice subjected to DSS colitis (7 days) followed by recovery from colitis (6 days). NPs and Ac2-26 peptide alone were administered only once via intraperitoneal injection (4 μg per mouse) at the first day of recovery (*$P < 0.001$). (**B**) Representative photomicrographs of hematoxylin and eosin–stained histological sections (original magnification, ×2). (**C**) Analysis of percentage of ulceration in whole colon samples (*$P = 0.0131$ vs. Scrm Ac2-26 Col IV NPs). (**D**) Fecal lipocalin analysis (*$P = 0.0037$ vs. Scrm Ac2-26 Col IV NPs; $n = 10$ mice per group). Quantitative data are expressed as mean ± SEM for each treatment group. Statistical comparisons were performed by ANOVA with Tukey's multiple comparison post-test.

ANXA1-containing EVs derived from the epithelium (27). Finally, the functional influence of EVs derived from ex vivo cultures on wound closure was assessed in a murine IEC line (CMT-93). Supporting our hypothesis, we observed increased wound repair mediated by *Anxa1*$^{+/+}$ EVs but not *Anxa1*$^{-/-}$ EVs (Figure 3D).

Taken together, these data suggest that ANXA1 is released as a component of EVs to promote wound repair.

ANXA1 in EVs is increased in the sera from patients with inflammatory bowel disease. Intestinal epithelial injury and mucosal inflammation are diagnostic pathologic features seen in patients with intestinal inflammatory disorders, such as inflammatory bowel disease (IBD). Since EVs are emerging as novel effectors of intertissue communication (10, 28), we hypothesized that increased ANXA1-containing EVs could be identified in the sera of patients with active IBD. Thus, we analyzed exosomes isolated from sera of individuals with IBD and healthy controls. Indeed, as shown in Figure 4, A and B, increased ANXA1 was detected in CD9- and ANXA5-containing exosomes isolated from individuals with active IBD compared with sera from healthy individuals. Supplemental Table 1 provides preoperative endoscopic findings and postoperative histologic diagnosis. For two patients with clinical diagnosis of acute colitis, no histologic scoring could be obtained, since no bowel specimen was resected. Concerning the diagnoses, some patients had active Crohn's disease, whereas others had active ulcerative colitis. Histologic examination of all surgical specimens revealed active mucosal inflammation. In our analysis, patients with high inflammatory activity also showed higher yields of ANXA1-containing EVs in their sera, as shown in the immunoblots in Figure 4B. However, diagnosis of Crohn's disease versus ulcerative colitis cannot be distinguished based on the immunoblotting results. These findings suggest that, while ANXA1-containing EVs in the serum correlate with the severity of acute mucosal inflammation, they do not distinguish the underlying mucosal disease.

Next, EVs in the serum were analyzed by flow cytometry using reference beads of known sizes, ranging from 1 μm to 50 nm (Figure 4, C–E). This analysis confirmed that increased ANXA1-containing EVs in the sera of patients with active IBD (Figure 4E) were derived in part from the epithelium (see Supplemental Figure 1F). Our findings are supportive of those of a previous study that reported endogenous ANXA1 secretion in the colons of human patients with ulcerative colitis (29).

Therapeutic administration of collagen IV–targeted polymeric NPs containing a ANXA1 mimetic peptide promotes recovery from dextran sulfate sodium colitis. To exploit the physiological mechanism of repair mediated by ANXA1-containing EVs, we investigated the therapeutic potential of targeted NPs containing the ANXA1 mimetic peptide Ac2-26 on mucosal repair in vivo. To

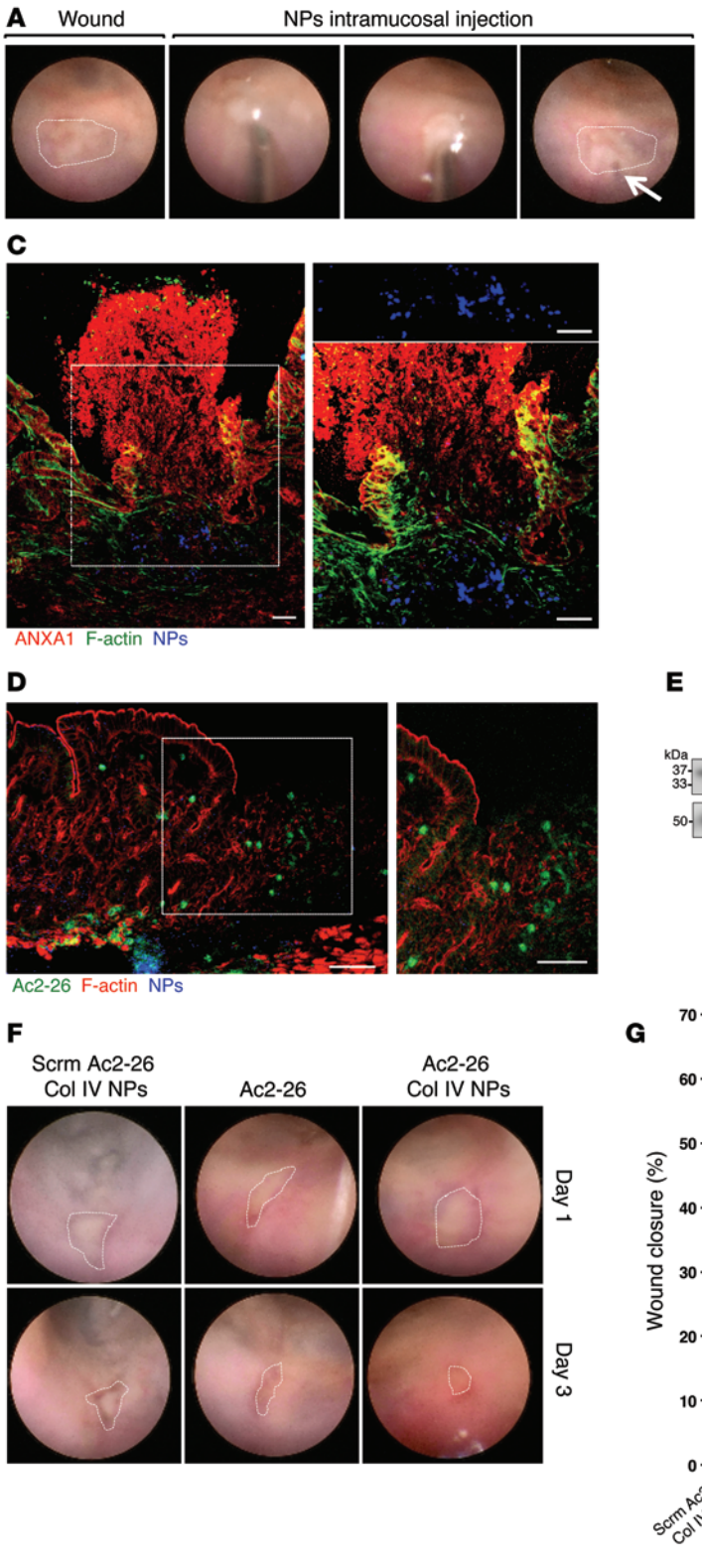

Figure 6. Intramucosal injections of Ac2-26 Col IV NPs augment colonic mucosal wound healing. (**A**) Images obtained during colonoscopy showing intramucosal injection of NPs in the mucosal wound bed. The arrow delineates the area of submucosal injection. (**B**) Schematic showing intramucosal NP injection into the colonic mucosal wounds. (**C**) Frozen sections of resealing colonic wounds in *Anxa1*$^{+/+}$ mice showing ANXA1 (red), F-actin (Alexa Fluor 488 phalloidin, green), and NPs (Alexa Fluor 647, blue). Higher-magnification images (original magnification, ×40) of the boxed region (original magnification, ×20) are shown to the right. Scale bar: 50 μm. (**D**) Frozen sections labeled for F-actin (Alexa Fluor 555 phalloidin, red). Released Ac2-26-FAM is shown in green and labeled Ac2-26 Col IV NPs are shown in blue. A higher-magnification image of the boxed region is shown to the right. Scale bar: 50 μm. (**E**) Immunoblot analysis of ANXA1 expression in nonwounded and resealing wounds of *Anxa1*$^{+/+}$ mice. Equivalent amounts of protein were loaded. From densitometry analysis ANXA1 protein in wounded tissue is increased versus nonwounded cells (2.568-fold increase, $P = 0.0005$, average of $n = 3$ immunoblots). (**F**) Endoscopic images of healing colonic mucosal wounds 1 or 3 days after biopsy-induced injury in *Anxa1*$^{-/-}$ mice treated with NPs. (**G**) Quantification of wound repair. Data are expressed as mean ± SEM; $n = 15$ mice per group. ***$P < 0.0001$ vs. Scrm Ac2-26 Col IV NPs and vs. Ac2-26. Statistical comparisons were performed by ANOVA with Tukey's multiple comparison post-test.

analyze mucosal repair from acute epithelial injury associated with mucosal inflammation, we used the murine dextran sulfate sodium (DSS) model of colitis (30). DSS was administered for 7 days and then withdrawn to allow recovery from colitis. The disease activity index was monitored over this entire period.

The NPs used in these experiments have previously been shown to have antiinflammatory properties (15). NPs were engineered to have a surface decorated with collagen IV, since it represents one of the main components of the basement membrane and therefore can enable targeting of NPs to vessels and injured

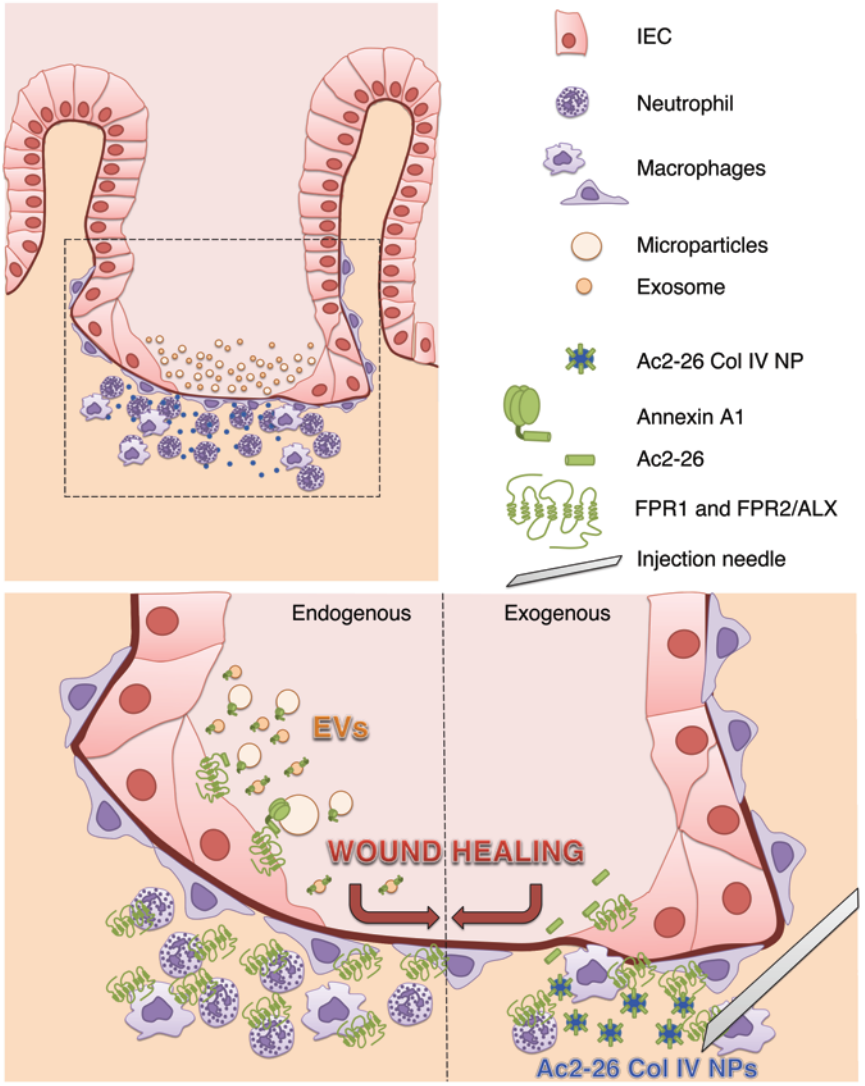

Figure 7. Endogenous epithelial-derived ANXA1-containing EVs and exogenous administration of Ac2-26 Col IV NPs activate FPRs to promote wound repair. Epithelial cells adjoining the wound flatten out, change polarity, and migrate as a sheet to cover denuded surfaces. Immune cells infiltrate into the site of injury in mucosal wounds. The healing epithelium is exposed to infiltrating immune cells that coordinate the mucosal repair. During this process, epithelial cells and immune cells release EVs (microparticles and exosomes) containing proresolution mediators, including ANXA1. ANXA1 in EVs signals through epithelial FPRs (FPR1 and FPR2/ALX) to promote wound repair (acting as an endogenous mediator of wound repair). This prorepair effect of endogenous ANXA1 can be mimicked using synthetically derived NPs containing ANXA1 mimetic peptide Ac2-26. Intramucosal injection of Ac2-26 Col IV NPs enhances epithelial wound healing (after exogenous administration of ANXA1).

mucosa (31). NPs containing a scrambled peptide (Scrm Ac2-26 Col IV NPs) and free Ac2-26 peptide were used as controls. To control for specificity of the exogenous Ac2-26–mediated effects, all in vivo experiments were performed in *Anxa1*$^{-/-}$ mice. In vitro, the NPs containing Ac2-26 (Ac2-26 Col IV NPs) showed increased IEC adherence and wound closure compared with those NPs containing Scrm Ac2-26 Col IV NPs, as shown in Supplemental Figure 2C. In vivo, Ac2-26 Col IV NPs, Scrm Ac2-26 Col IV NPs, and Ac2-26 alone were administered by intraperitoneal injection on the first day of recovery (Figure 5A). A single injection of Ac2-26 Col IV NPs promoted repair of the intestinal mucosa, as judged by the disease activity index, compared with Scrm Ac2-26 Col IV NPs or Ac2-26 alone (Figure 5, A–C).

Histological analysis confirmed decreased intestinal mucosal ulceration in mice treated with Ac2-26 Col IV NPs. Similarly, fecal lipocalin-2, used as an inflammatory marker, was also reduced in mice administered Ac2-26 Col IV NPs compared with that in those administered Scrm Ac2-26 Col IV NPs or Ac2-26 alone (Figure 5D and ref. 32). Altogether, these results suggest that a single administration of Ac2-26 Col IV NPs mediates a potent and sustained effect on recovery from acute colitis.

Intramucosal administration of Ac2-26 NPs accelerates intestinal mucosal wound healing. A major advantage of using NPs is that they can provide a platform for sustained and direct release of the proresolving peptide (Ac2-26) at the site of administration. To further demonstrate this beneficial effect, we investigated the influence of NPs on healing of intestinal mucosal biopsy-induced wounds in WT mice generated using a mouse colonoscope (7, 26). A single intramucosal injection of NPs or Ac2-26 peptide alone into the wound bed was performed (Figure 6, A and B, and Supplemental Video 1), and wound healing was analyzed 3 days later. As shown in Figure 6, C and D, fluorescent NPs and labeled peptide Ac2-26 released from NPs could be identified in the wound bed 3 days after administration. Since endogenous ANXA1 protein was increased in resealing mucosal wounds 3 days after injury (Figure 6E), we next examined the influence of intramucosal delivery of Ac2-26 Col IV NPs into intestinal mucosal wounds in ANXA1-deficient mice. In keeping with improved recovery from DSS colitis, intramucosal administration of Ac2-26 Col IV NPs increased wound repair compared with administration of Scrm Ac2-26 Col IV NPs or a single injection of Ac2-26 peptide (Ac2-26 Col IV NPs: 62.96% ± 3.08% vs. Scrm Ac2-26 Col IV NPs: 29.15% ± 3.6%, $P < 0.0001$; Figure 6, F and G).

Discussion

Timely and efficient intestinal mucosal wound repair, coinciding with resolution of inflammation, is critical in reestablishing the epithelial barrier and mucosal homeostasis. We and others have shown that ANXA1 and its N-terminal peptide, Ac2-26, have epithelial prorepair properties that require the activation of FPRs (4, 5, 7). Resolution of inflammation and repair of the epithelial barrier are mediated by a delicate choreography of mediators derived from the epithelium as well as by inflammatory cells in the lamina propria of the mucosa. Thus, an improved understanding of these biological processes is important in development of therapeutic strategies designed to promote recovery of epithelial injury in inflammatory states such as IBD (1, 33).

Recent studies have identified a number of mediators that play an active role in the resolution of inflammation, including ANXA1, lipoxins, resolvins, protectins, and maresins (3, 34–37). ANXA1 is expressed by a number of cell types, including epithelial cells and phagocytes, and mediates its biological responses by activating FPRs that are expressed in both phagocytes and epithelial cells. Three FPRs (FPR1, FPR2/ALX, and FPR3) have been identified in humans (38). The ANXA1 N-terminal peptide, Ac2-26, preferentially associates with epithelial FPR1 to promote intestinal wound repair (7, 23). In this study, we report that ANXA1 is released from IECs as a component of EVs and that these EVs possess prorepair properties. Remarkably, EVs derived from *Anxa1*$^{-/-}$ mice failed to enhance epithelial wound healing. A schematic representation of our results is shown in Figure 7. Endogenous ANXA1 released in EVs from epithelial cells and leukocytes after injury orchestrates epithelial wound repair. Furthermore, in vivo, local administration of synthetic NPs containing Ac2-26 mimics the prorepair effects of epithelial and immune cell–derived EVs. Additionally, a previous study reported ANXA1 association with the exoplasmic surface of vesicles secreted by prostate epithelial cells into the seminal fluid or prostasomes may contribute to suppression of the immune response in the female reproductive tract (39).

The extracellular influence of ANXA1 is regulated by proteolytic cleavage of the N terminus of the protein by MMPs. Increased MMP activity has been identified in inflamed tissues and such MMP activity has been reported to dampen inflammation by promoting cleavage of chemokines (16, 40). Given this scenario, one can envision that increased MMPs facilitate resolution of inflammation both by promoting cleavage of ANXA1 and release of the N-terminal peptide, Ac2-26 (7, 41–46). Pharmacological inhibition of MMP9 markedly reduced ANXA1 detection in EVs (Supplemental Figure 1, A and B). MMP9 activation during inflammation is therefore likely to play an important role in ANXA1 proteolysis. Upon cellular activation, ANXA1 is released from its storage sites and translocates immediately to the membrane. In neutrophils, ANXA1 is stored in gelatinase granules, and upon neutrophil-activating events, such as adhesion to the endothelium, it is rapidly exteriorized (47), exposing the N-terminal region that mediates its biological response (Figure 3D). Neutrophil ANXA1 externalization can occur without interaction with endothelial cells, indicating that cellular adhesion to the endothelium is not required for release of ANXA1 (48). For the first time to our knowledge, we show that epithelial-derived ANXA1-containing EV release is highly regulated by wounding (as shown in Figure 3B). Furthermore, ANXA1 in epithelial-derived EVs is in large part distributed on the surface of cells (Supplemental Figure 2A).

FPR1 and FPR2/ALX, receptors for ANXA1 and ANXA1 mimetic peptide Ac2-26, are localized in both the luminal apical plasma membrane as well as in the basolateral membrane of IECs. After tissue injury the polarity of epithelial cells that migrate as a sheet to cover denuded mucosal surfaces is changed. Epithelial cells at the leading edge flatten out, and a clear distinction between apical and basolateral plasma membrane is not evident. ANXA1 that is exteriorized and released in EVs binds and activates FPRs in the plasma membrane of the migrating sheet of epithelial cells.

Importantly, recent studies have highlighted a role of EVs released from cells in mediating cross talk between different cell types (10, 28). Macrophages reside in close proximity to the repairing epithelium and have been shown to attenuate the immune response while also promoting the extracellular matrix remodeling required for wound repair (49). Furthermore, macrophages generate maresins that exert proresolving effects in inflammation (50, 51). In addition to macrophages, neutrophils in wounds shed microparticles containing ANXA1 that activate FPRs in leukocytes (8) as well as in the epithelium to promote resolution of inflammation and repair. A recent study reported a novel approach using human polymorphonuclear cell–derived microparticles enriched in resolvin D1 and lipoxin A_4 analogs in facilitating resolution of inflammation in murine peritonitis (52).

IBD is pathologically characterized by mucosal inflammation and, during active phases of the disease, by infiltration of neutrophils and mucosal ulceration (53, 54). To determine whether ANXA1-containing EVs could serve as a biomarker of active IBD, we analyzed EVs in the sera of healthy controls and patients with IBD. Disease severity was assessed clinically and endoscopically and by histologic analysis of resected surgical specimens where applicable (see Supplemental Table 1). All patients presented clinical signs of acute disease of different levels of severity. Patients with increased active mucosal inflammation exhibited elevated ANXA1-containing EVs in the sera compared with patients with milder disease activity. However, we detected ANXA1-containing EVs in all patients with active mucosal inflammation. Since a previous study has reported expression of ANXA1 by neutrophil-derived EVs (8), we predict that in the local microenvironment of the wound, ANXA1-containing EVs might be derived not only from infiltrating leukocytes but also from the repairing epithelium. In fact, we demonstrated the presence of ANXA1-containing EVs that colabeled with an epithelial-derived protein, A33, in ex vivo cultures of wounds (55). In conclusion, detection of ANXA1-containing EVs in the serum could serve as a biomarker for active mucosal inflammation (56).

NPs can be used as a pharmacological approach that can improve bioavailability and tissue distribution and half-life of the administered agent and minimize systemic undesired effects and therefore have therapeutic potential for use in wound repair associated with inflammation as well as in tissue regeneration. In our study, the therapeutic effects of Ac2-26 Col IV NPs were tested in two injury and inflammation models that include recovery from DSS colitis and resealing of colonic biopsy-induced wounds. These models are amenable to detailed morphological analysis of resolution of mucosal inflammation and repair of the intestinal epithe-

lium. In addition to systemic administration, local intramucosal delivery of Ac2-26 Col IV NPs, recently tested in vivo in zymosan-induced peritonitis and murine models of ischemia-reperfusion injury, was sufficient in promoting colonic mucosal wound repair (15). NPs used as peptide carriers are highly stable and therefore require reduced peptide dosing, demonstrating that this mode of administration is a technological advance. In addition, the choice of encapsulation of Ac2-26 versus the whole protein was based on the fact that ANXA1 is highly susceptible to proteolytic cleavage within the N terminus by MMPs in the injured mucosa. Furthermore, NPs injected via the intramucosal route, as presented in our study, restricted access of the Ac2-26 peptide to specific sites of wounded colonic mucosa, thereby delivering the prorepair peptide at a controlled and sustained rate (over 4 days). Furthermore, the NPs were not eliminated from the intestine by diarrhea that is associated with mucosal inflammation and injury (57, 58). Thus, this mode of therapy represents an advance in the current experimental approaches used in nanomedicine (57, 58). While our study focused on the intestinal tract, NP-mediated delivery of therapeutic peptides is likely a viable strategy that can be used in promoting repair of other epithelial surfaces, such as the skin and lung. Given the easy access to skin wounds, local delivery to injured sites is a feasible option. Additionally, the delivery of NPs into injured respiratory mucosa by aerosolization would be a potential approach that could to be explored in future studies. The development and engineering of NPs containing proresolving compounds may thus establish a new modality of intercellular communication aimed to resolve inflammation and repair epithelial barriers.

Methods

Study design. The first objective of this study was to investigate the mechanisms by which ANXA1 is released from the cell surface in EVs to activate FPRs and promote intestinal epithelial wound repair. As the second objective, therapeutic effects of Ac2-26 Col IV NPs were investigated both following endoscopic biopsy of colonic mucosa and during recovery from DSS colitis. Ac2-26 Col IV NPs were injected into the colonic mucosa of biopsy-generated wounds in *Anxa1*$^{-/-}$ mice. Intraperitoneal injections were performed in *Anxa1*$^{-/-}$ mice with colitis. Parameters for epithelial wound repair were analyzed after 3 days of healing in the colonoscopy model (percentage of wound closure) and following 6 days of recovery in the colitis model (disease activity index). Study design and sample sizes were predetermined on the basis of previous experience (7), using at minimum 5 mice per group, and all experiments were replicated at least 3 times to confirm findings. Mice were randomly assigned to treatment groups, and where possible, treatment groups were blinded until statistical analysis. No potential outliers were excluded from the data sets presented in this study.

Antibodies and reagents. Antibodies to CD9 (catalog no. ab92726), CD63 (catalog no. ab134045), ANXA5 (catalog no. ab14196), CD151 (catalog no. ab185684), and ADAM-10 (catalog no. ab1997) were purchased from abcam; MMP2 (catalog no. 4022) and MMP9 (catalog no. 3852) from Cell Signaling; and monoclonal anti–α-tubulin antibody produced in mouse (catalog no. T9026) from Sigma-Aldrich. Flotillin-1 antibody (catalog no. 610821) and ANXA1 inhibitory antibody (clone 29, catalog no. 610066) were purchased from BD Transduction Laboratories. Mouse IgG1 control antibody (catalog no. 02-6100), anti-ANXA1 antibody (catalog no. 71-3400), TRITC-labeled phalloidin (catalog no. R415), Exosome-Dynabeads Human CD63 Isolation/Detection (catalog no. 10606D), ExoQuick serum exosome precipitation solution (catalog no. EXOQ5A-1), and BCECF, AM (catalog no. B-1150) were purchased from Life Technologies (Invitrogen). EpCAM magnetic beads (catalog no. 130-061-10) were purchased from Miltenyi Biotec. Hydro-Cy3 Dye (product no. 926-20000; product name: ROSstar 550 Probe) was purchased from LI-COR. Compound GI254023X (catalog no. 3995) was purchased from Tocris; TAPI-2 (catalog no. 579052) and MMP9 II inhibitor (catalog no. 444293) were purchased from EMD Millipore; and Cyclosporin H (catalog no. ALX-380-286-M001) was purchased from EnzoLife Bioscience. BAPTA-AM (catalog no. 2787), ML-7 (catalog no. 4310), Y-27632 (catalog no. 1254), Dynasore (catalog no. 2897), Cytochalasin D (catalog no. 1233), Jasplakinolide (catalog no. 2792), WRW4 (catalog no. 2262), and ANXA5 (catalog no. 10448-HNAE) were purchased from Invitrogen. Z-VAD-FMK (catalog no. 187389-52-2) was purchased from Santa Cruz Biotechnology. Cytokines (IL-1β, IFN-γ, and TNF-α) were obtained by Peprotech. Human recombinant ANXA1 (hrANXA1) was purified as previously reported (7).

Mice. Wild-type mice were purchased from The Jackson Laboratory. *Anxa1*$^{-/-}$ mice were generated as previously described (63).

Cell lines and culture conditions. IECs (SK-CO15 [human] and CMT-93 [murine]) were obtained from the Digestive Diseases Research Development Center Cell Culture Core (Emory University, Atlanta, Georgia, USA). SK-CO15 cells were grown in high glucose (4.5 g/l), DMEM supplemented with 10% FBS, 100 units/ml penicillin, 100 μg/ml streptomycin, 15 mm HEPES (pH 7.4), 2 mm L-glutamine, and 1% nonessential amino acids, as described previously (59), at 37°C in a 4% CO_2 incubator.

Polymeric Ac2-26 Col IV NPs. Targeted polymeric Ac2-26 Col IV NPs and Scrm Ac2-26 Col IV NPs were made and characterized according to previously published protocols (15). NPs were labeled with Alexa Fluor 647 and fluorescent Ac2-26-FAM for detection at the site of injection.

DSS colitis. Mice were allowed free access to food and drinking water containing 3% (w/v) DSS for 7 days, and recovery was allowed for additional 6 days. Daily clinical assessment and histological analysis were performed as previously described (60, 61).

Confocal immunofluorescence microscopy. Tissue was fixed with 3.7% (w/v) paraformaldehyde at room temperature for 15 minutes, followed by 0.5% (w/v) Triton X-100 for 5 minutes. Primary antibody incubation was performed overnight. Images were taken on an LSM 510 confocal microscope (Zeiss).

Wound healing assay. Cell migration was assessed using a scratch wound assay as previously published (59). Inhibitors were added 30 minutes prior to the mechanical wound injury. In some experiments, epithelial cells were incubated with EVs (2 μg) or hrANXA1 (10 nM). For immunoblot analysis, confluent cell monolayers grown in 6-well tissue culture plates were scraped 8 times horizontally and vertically to enrich for migrating cells.

Cell surface biotinylation. IECs were plated in a 6-well plate and incubated on ice in PBS containing 500 μg/ml sulfo-NHS-biotin. After aspiration, cells were washed twice with 10 mM Tris-HCl, pH 7.2, and 150 mM NaCl to quench the biotinylation reaction. Scratch wound assay was performed. After 4 hours, wound healing the supernatant was incubated with avidin-coated agarose beads overnight. Immunoprecipitates of biotinylated surface proteins bound to avidin-agarose were washed 5 times in RIPA buffer and analyzed for ANXA1 using the immunoblot technique.

EVs purification and analysis. EVs were isolated and purified using a previously published protocol (62). Culture medium was subjected to differential centrifugation to remove cells, dead cells, and cell debris at a rate of 20,000 *g* for 20 minutes (microparticles isolation) to 100,000 *g* (for exosome isolation) for 60 minutes. The amount of proteins recovered was measured by Bradford assay. For immunoblot analysis, EVs were washed once with HBSS and resuspended in RIPA lysis buffer. EVs were prepared for ImageStream^X Imaging Flow Cytometry analysis as previously described (22). EVs were stained with 25 μM BODIPY-Texas Red dye, 0.5 μg/ml anti-ANXA1 mAb (clone 1B; Alexa Fluor 488 conjugated; produced in-house using a APEX Alexa Fluor 488 Antibody Labeling Kit [catalog no. A10468] from Invitrogen), anti-CD11b PE (eBioscience), and anti-A33 (R&D Systems) antibodies. All staining was carried out at 4°C in the dark for 30 minutes. Immediately prior to acquiring each sample, 1-μm and 500-nm fluorescent reference beads (catalog no. L1278-1ML and L1403-1ML, respectively; Sigma-Aldrich) were added to a final concentration of 1 in 6 from stock. All samples were acquired on the ImageStream^X MkII (Amnis Corp.) at low flow rate, ×60 magnification, and all lasers (488 nm, 405 nm, 633 nm, and 785 nm) at full voltage. Two separate samples containing 1× 100-nm beads and 1× 50-nm beads (catalog no. L1528-1ML and L0780-1ML, respectively; Sigma-Aldrich) were run to generate overlays with EV populations. Isotype control samples for in vivo and in vitro data as well as single-color stains for compensation were acquired as appropriate. ImageStream data were acquired using INSPIRE and analyzed using IDEAS. Sera from patients with IBD and healthy individuals were incubated overnight with EpCAM magnetic beads (Miltenyi Biotec), followed by immunoblotting.

Detection of ANXA1-containing EVs in sera of patients with active IBD. For detection of EVs containing ANXA1, sera of patients with active ulcerative colitis or Crohn's disease was obtained during hospitalization of the patients. Except for one patient that did not undergo surgery, all samples were taken preoperatively. Details regarding disease severity, preoperative endoscopic findings and postoperative histologic diagnosis are shown in Supplemental Table 1. No histologic analysis was obtained for 2 patients, because one patient was treated medically and, in the other case, no bowel specimen was removed, but both were diagnosed clinically. Healthy non-IBD individuals with no other known diseases were used as controls. For isolation of EVs from the serum SBI's Serum ExoQuick precipitation reagent was used.

Detection of intracellular ROS. This was performed as previously described (7).

Colonoscopy in live mice. Mice were anesthetized by intraperitoneal injection of a ketamine (10 g/l)/xylazine (8 g/l) solution (10 μl/g body weight). To create mucosal injuries in the mouse colon and to monitor their regeneration, a high-resolution colonoscopy system was used. Each wound region was digitally photographed at day 1 and day 3, and wound areas were calculated using ImageJ software. In each experiment, 3 to 4 lesions per mouse were examined (7).

Quantification of fecal Lcn-2 by ELISA. Lcn-2 levels were estimated in the supernatants of freshly collected fecal samples reconstituted in PBS containing 0.1% Tween 20 (100 mg/ml) using the Duoset Murine Lcn-2 ELISA Kit (R&D Systems).

Electron microscopy. EVs were suspended in PBS and fixed by adding an equal volume of 2% paraformaldehyde in 0.1 M phosphate buffer (pH 7.4). EVs were absorbed for 10 minutes by 400-mesh carbon-coated copper grids by floating the grids on 10 μl drops on parafilm. Grids with adhered EVs were briefly washed by touching the side of grid with EVs to a drop of double-distilled water. For negative staining, 5 μl 1% aqueous phosphotungstic acid (pH 6.5) was applied onto the vesicles on the grid immediately after water removal and then removed as described above after 30 seconds. The grid was allowed to dry completely before viewing on a JEOL JEM-1400 transmission electron microscope (JEOL Ltd.) equipped with a Gatan US1000, 2k × 2k CCD camera (Gatan Inc.). Immunogold labeling was performed at room temperature by floating the grids on drops containing the diluted anti-ANXA1, CD9, and ANXA5 primary antibodies. After several buffer washes, the grids were floated on drops of 10 nm colloidal gold particle–conjugated secondary antibodies for 1 hour.

Ex vivo culture of murine mucosal colonic wounds. Mouse colonic small tissue biopsies (4 mm) containing the wounds (obtained by colonoscopy technique) were removed with a punch biopsy instrument. Tissues were rinsed with sterile PBS to remove cellular debris and immediately placed into a 24-well culture plate (3 wounds from each mouse per well). Cultures were maintained for 4 hours at 37°C, 5% CO_2, supernatants were collected, and EVs were isolated.

Statistics. Statistical comparisons were performed by either Student's 2-tailed *t* test or ANOVA with Tukey multiple comparison post-test, as appropriate. A *P* value of less than 0.05 was considered significant.

Study approval. Informed consent was obtained from all patients and healthy controls, and research on the obtained samples was performed in accordance with institutional review board approval from the University of Muenster (approval no. "1IXHai"). All animal experiments were approved by the Institutional Animal Care and Use Committee at Emory University and performed according to NIH guidelines.

Acknowledgments

The authors thank Hong Pang at the Cell Culture Core Facility and Hong Yi and Elizabeth Wright at the Emory Electron Microscopy Core. This work was supported by NIH grants (RO1DK089763 to A. Nusrat and A.S. Neish; RO1DK055679 to A. Nusrat; RO1AI64462 to A.S. Neish; and DK061379, DK072564, DK079392 to C.A. Parkos); the German Research Foundation (Deutsche Forschungsgemeinschaft, Bonn, Germany, NE1834/1-1 to P.A. Neumann); the William Harvey Research Foundation (to M. Perretti); the Wellcome Trust (equipment grant 10160Z13Z); and the Emory Digestive Diseases Research Development Center Core Grant (DK 064399). This work was also supported by a Program of Excellence in Nanotechnology award, contract no. HHSN268201000045C, from the National Heart, Lung, and Blood Institute, NIH.

Address correspondence to: Asma Nusrat, Epithelial Pathobiology and Mucosal Inflammation Research Unit, Department of Pathology and Laboratory Medicine, 105-M Whitehead Bldg., 615 Michael St., Atlanta, Georgia 30322, USA. Phone: 404.727.8543; E-mail: anusrat@emory.edu. Or to: Andrew S. Neish, Epithelial Pathobiology and Mucosal Inflammation Research Unit, Department of Pathology and Laboratory Medicine, 105-L Whitehead Bldg., 615 Michael St., Atlanta, Georgia 30322, USA. Phone: 404.727.8545; E-mail: aneish@emory.edu. Or to: Omid C. Farokhzad, Brigham and Women's Hospital Neville House, 75 Francis Street, Boston, Massachusetts 02115, USA. Phone: 617.732.6093; E-mail: ofarokhzad@zeus.bwh.harvard.edu.

1. Koch S, Nusrat A. The life and death of epithelia during inflammation: lessons learned from the gut. *Annu Rev Pathol*. 2012;7:35–60.
2. Serhan CN, Dalli J, Colas RA, Winkler JW, Chiang N. Protectins and maresins: new pro-resolving families of mediators in acute inflammation and resolution bioactive metabolome [published online ahead of print August 17, 2014]. *Biochim Biophys Acta*. doi:10.1016/j.bbalip.2014.08.006.
3. Serhan CN. Pro-resolving lipid mediators are leads for resolution physiology. *Nature*. 2014;510(7503):92–101.
4. Babbin BA, et al. Annexin I regulates SKCO-15 cell invasion by signaling through formyl peptide receptors. *J Biol Chem*. 2006; 281(28):19588–19599.
5. Martin GR, Perretti M, Flower RJ, Wallace JL. Annexin-1 modulates repair of gastric mucosal injury. *Am J Physiol Gastrointest Liver Physiol*. 2008;294(3):G764–G769.
6. Perretti M, D'Acquisto F. Annexin A1 and glucocorticoids as effectors of the resolution of inflammation. *Nat Rev Immunol*. 2009;9(1):62–70.
7. Leoni G, et al. Annexin A1, formyl peptide receptor, and NOX1 orchestrate epithelial repair. *J Clin Invest*. 2013;123(1):443–454.
8. Dalli J, Norling LV, Renshaw D, Cooper D, Leung KY, Perretti M. Annexin 1 mediates the rapid anti-inflammatory effects of neutrophil-derived microparticles. *Blood*. 2008;112(6):2512–2519.
9. Dalli J, Serhan CN. Specific lipid mediator signatures of human phagocytes: microparticles stimulate macrophage efferocytosis and pro-resolving mediators. *Blood*. 2012;120(15):e60–e72.
10. Raposo G, Stoorvogel W. Extracellular vesicles: exosomes, microvesicles, and friends. *J Cell Biol*. 2013;200(4):373–383.
11. Thery C, Zitvogel L, Amigorena S. Exosomes: composition, biogenesis and function. *Nat Rev Immunol*. 2002;2(8):569–579.
12. van Niel G, et al. Intestinal epithelial cells secrete exosome-like vesicles. *Gastroenterology*. 2001;121(2):337–349.
13. Cocucci E, Racchetti G, Meldolesi J. Shedding microvesicles: artefacts no more. *Trends Cell Biol*. 2009;19(2):43–51.
14. Caby MP, Lankar D, Vincendeau-Scherrer C, Raposo G, Bonnerot C. Exosomal-like vesicles are present in human blood plasma. *Int Immunol*. 2005;17(7):879–887.
15. Kamaly N, et al. Development and in vivo efficacy of targeted polymeric inflammation-resolving nanoparticles. *Proc Natl Acad Sci U S A*. 2013;110(16):6506–6511.
16. Khokha R, Murthy A, Weiss A. Metalloproteinases and their natural inhibitors in inflammation and immunity. *Nat Rev Immunol*. 2013;13(9):649–665.
17. Trajkovic K, et al. Ceramide triggers budding of exosome vesicles into multivesicular endosomes. *Science*. 2008;319(5867):1244–1247.
18. Escola JM, Kleijmeer MJ, Stoorvogel W, Griffith JM, Yoshie O, Geuze HJ. Selective enrichment of tetraspan proteins on the internal vesicles of multivesicular endosomes and on exosomes secreted by human B-lymphocytes. *J Biol Chem*. 1998;273(32):20121–20127.
19. Bi GQ, Alderton JM, Steinhardt RA. Calcium-regulated exocytosis is required for cell membrane resealing. *J Cell Biol*. 1995;131(6 pt 2):1747–1758.
20. Gerke V, Creutz CE, Moss SE. Annexins: linking Ca^{2+} signalling to membrane dynamics. *Nat Rev Mol Cell Biol*. 2005;6(6):449–461.
21. Fenteany G, Zhu S. Small-molecule inhibitors of actin dynamics and cell motility. *Curr Top Med Chem*. 2003;3(6):593–616.
22. Headland SE, Jones HR, D'Sa AS, Perretti M, Norling LV. Cutting-edge analysis of extracellular microparticles using ImageStream(X) imaging flow cytometry. *Sci Rep*. 2014;4:5237.
23. Babbin BA, et al. Annexin A1 regulates intestinal mucosal injury, inflammation, and repair. *J Immunol*. 2008;181(7):5035–5044.
24. McNeil AK, Rescher U, Gerke V, McNeil PL. Requirement for annexin A1 in plasma membrane repair. *J Biol Chem*. 2006;281(46):35202–35207.
25. Kundu K, Knight SF, Willett N, Lee S, Taylor WR, Murthy N. Hydrocyanines: a class of fluorescent sensors that can image reactive oxygen species in cell culture, tissue, and in vivo. *Angew Chem Int Ed Engl*. 2009;48(2):299–303.
26. Becker C, Fantini MC, Neurath MF. High resolution colonoscopy in live mice. *Nat Protoc*. 2006;1(6):2900–2904.
27. Moritz RL, et al. Micro-sequencing strategies for the human A33 antigen, a novel surface glycoprotein of human gastrointestinal epithelium. *J Chromatogr A*. 1998;798(1–2):91–101.
28. Buzas EI, György B, Nagy G, Falus A, Gay S. Emerging role of extracellular vesicles in inflammatory diseases. *Nat Rev Rheumatol*. 2014;10(6):356–364.
29. Vergnolle N, et al. Annexin 1 is secreted in situ during ulcerative colitis in humans. *Inflamm Bowel Dis*. 2004;10(5):584–592.
30. Wirtz S, Neufert C, Weigmann B, Neurath MF. Chemically induced mouse models of intestinal inflammation. *Nat Protoc*. 2007;2(3):541–546.
31. Chan JM, et al. Spatiotemporal controlled delivery of nanoparticles to injured vasculature. *Proc Natl Acad Sci U S A*. 2010;107(5):2213–2218.
32. Chassaing B, Srinivasan G, Delgado MA, Young AN, Gewirtz AT, Vijay-Kumar M. Fecal lipocalin 2, a sensitive and broadly dynamic non-invasive biomarker for intestinal inflammation. *PLoS One*. 2012;7(9):e44328.
33. Cordeiro JV, Jacinto A. The role of transcription-independent damage signals in the initiation of epithelial wound healing. *Nat Rev Mol Cell Biol*. 2013;14(4):249–262.
34. Spite M, Claria J, Serhan CN. Resolvins, specialized proresolving lipid mediators, and their potential roles in metabolic diseases. *Cell Metab*. 2014;19(1):21–36.
35. Abdulnour RE, et al. Maresin 1 biosynthesis during platelet-neutrophil interactions is organ-protective. *Proc Natl Acad Sci U S A*. 2014;111(46):16526–16531.
36. Buckley CD, Gilroy DW, Serhan CN. Proresolving lipid mediators and mechanisms in the resolution of acute inflammation. *Immunity*. 2014;40(3):315–327.
37. Fredman G, et al. Resolvin D1 limits 5-lipoxygenase nuclear localization and leukotriene B4 synthesis by inhibiting a calcium-activated kinase pathway. *Proc Natl Acad Sci U S A*. 2014;111(40):14530–14535.
38. Ye RD, et al. International Union of Basic and Clinical Pharmacology. LXXIII. Nomenclature for the formyl peptide receptor (FPR) family. *Pharmacol Rev*. 2009;61(2):119–161.
39. Aalberts M, et al. Identification of distinct populations of prostasomes that differentially express prostate stem cell antigen, annexin A1, and GLIPR2 in humans. *Biol Reprod*. 2012;86(3):82.
40. Van Lint P, Libert C. Chemokine and cytokine processing by matrix metalloproteinases and its effect on leukocyte migration and inflammation. *J Leukoc Biol*. 2007;82(6):1375–1381.
41. Brancaleone V, Dalli J, Bena S, Flower RJ, Cirino G, Perretti M. Evidence for an anti-inflammatory loop centered on polymorphonuclear leukocyte formyl peptide receptor 2/lipoxin A4 receptor and operative in the inflamed microvasculature. *J Immunol*. 2011;186(8):4905–4914.
42. Hayhoe RP1, Kamal AM, Solito E, Flower RJ, Cooper D, Perretti M. Annexin 1 and its bioactive peptide inhibit neutrophil-endothelium interactions under flow: indication of distinct receptor involvement. *Blood*. 2006;107(5):2123–2130.
43. Bena S, Brancaleone V, Wang JM, Perretti M, Flower RJ. Annexin A1 interaction with the FPR2/ALX receptor: identification of distinct domains and downstream associated signaling. *J Biol Chem*. 2012;287(29):24690–24697.
44. Cooray SN, et al. Ligand-specific conformational change of the G-protein-coupled receptor ALX/FPR2 determines proresolving functional responses. *Proc Natl Acad Sci U S A*. 2013;110(45):18232–18237.
45. Alam A, et al. Redox signaling regulates commensal-mediated mucosal homeostasis and restitution and requires formyl peptide receptor 1. *Mucosal Immunol*. 2014;7(3):645–655.
46. Gronert K, Maheshwari N, Khan N, Hassan IR, Dunn M, Laniado Schwartzman M. A role for the mouse 12/15-lipoxygenase pathway in promoting epithelial wound healing and host defense. *J Biol Chem*. 2005;280(15):15267–15278.
47. Perretti M, Flower RJ. Measurement of lipocortin 1 levels in murine peripheral blood leukocytes by flow cytometry: modulation by glucocorticoids and inflammation. *Br J Pharmacol*. 1996;118(3):605–610.
48. Vong L, et al. Annexin 1 cleavage in activated neutrophils: a pivotal role for proteinase 3. *J Biol Chem*. 2007;282(41):29998–30004.
49. Mosser DM, Edwards JP. Exploring the full spectrum of macrophage activation. *Nat Rev Immunol*. 2008;8(12):958–969.
50. Dalli J, et al. The novel 13S,14S-epoxy-maresin is converted by human macrophages to maresin 1 (MaR1), inhibits leukotriene A4 hydrolase (LTA4H), and shifts macrophage phenotype. *FASEB J*. 2013;27(7):2573–2583.
51. Serhan CN, et al. Macrophage proresolving mediator maresin 1 stimulates tissue regeneration and controls pain. *FASEB J*. 2012;26(4):1755–1765.
52. Norling LV, Spite M, Yang R, Flower RJ, Perretti M, Serhan CN. Cutting edge: Humanized nano-proresolving medicines mimic inflammation-resolution and enhance wound healing. *J Immunol*. 2011;186(10):5543–5547.
53. Baumgart DC, Sandborn WJ. Crohn's disease.

Lancet. 2012;380(9853):1590–1605.
54. Ordás I, Eckmann L, Talamini M, Baumgart DC, Sandborn WJ. Ulcerative colitis. *Lancet*. 2012;380(9853):1606–1619.
55. Tauro BJ, Greening DW, Mathias RA, Mathivanan S, Ji H, Simpson RJ. Two distinct populations of exosomes are released from LIM1863 colon carcinoma cell-derived organoids. *Mol Cell Proteomics*. 2013;12(3):587–598.
56. Buzas EI, György B, Nagy G, Falus A, Gay S. Emerging role of extracellular vesicles in inflammatory diseases. *Nat Rev Rheumatol*. 2014;10(6):356–364.
57. Ulbrich W, Lamprecht A. Targeted drug-delivery approaches by nanoparticulate carriers in the therapy of inflammatory diseases. *J R Soc Interface*. 2010;7(suppl 1):S55–S66.
58. Laroui H, et al. Nanomedicine in GI. *Am J Physiol Gastrointest Liver Physiol*. 2011;300(3):G371–G383.
59. Babbin BA, et al. Formyl peptide receptor-1 activation enhances intestinal epithelial cell restitution through phosphatidylinositol 3-kinase-dependent activation of Rac1 and Cdc42. *J Immunol*. 2007;179(12):8112–8121.
60. Khounlotham M, et al. Compromised intestinal epithelial barrier induces adaptive immune compensation that protects from colitis. *Immunity*. 2012;37(3):563–573.
61. Nava P, et al. Interferon-γ regulates intestinal epithelial homeostasis through converging β-catenin signaling pathways. *Immunity*. 2010;32(3):392–402.
62. Théry C, Amigorena S, Raposo G, Clayton A. Isolation and characterization of exosomes from cell culture supernatants and biological fluids. *Curr Protoc Cell Biol*. 2006;Chapter 3:Unit 3.22.
63. Hannon R, et al. Aberrant inflammation and resistance to glucocorticoids in annexin $1^{-/-}$ mouse. *FASEB J*. 2003;17(2):253–255.